CHAPTER IV

RESULTS AND DISCUSSION

4.1 Synthesis of Cassiarin A (4)

Synthesis of **4** was performed following two synthetic approaches starting from Scheme 4-9. The first one was stepwise synthesis via the formation of 5-acetonyl-7-hydroxy-2-methyl chromone (**27**). The second one was direct synthesis of **4** from **1**.

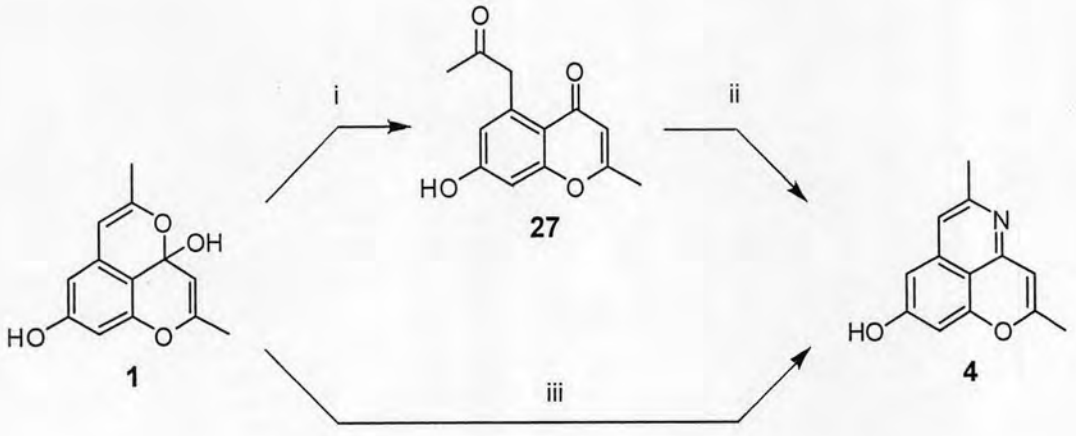

conditions: i) TEA, MeOH/H_2O, rt, 12 h, 32%, ii) NH_4OAc, glac. AcOH, reflux, 4–5 h, 58%, iii) NH_4OAc or NH_4Cl, MeOH, reflux, 4–5 h, 57–67%.

Scheme 4-9. Synthesis of **4** from the reaction of **1** and **27** with ammonium acetate.

In the first approach, compound **1** was reacted with triethylamine in the aqueous methanol at room temperature for 12 h to give **27** in 32% yield. Chromone **27** was then converted to **4** by a reaction with ammonium acetate in glacial acetic acid under reflux for 4–5 h, affording **4** in 58% yield. In the second approach, compound **4** was directly synthesized by a reaction of **1** and ammonium acetate in methanol under reflux for 4–5 h, leading to **4** in 57% yield. When ammonium chloride was used instead of ammonium acetate, the yield of the desirable product **4** was increased to 67%. To obtain a practical

synthesis procedure applicable for the preparation of both **4** and **5** [13], another synthesis approach was pursued and schematically shown in Scheme 4-10. Compound **1** was reacted with concentrated hydrochloric acid in methanol or ethanol to produce compound **3** in 58% isolated yield. Compound **3** served as a key precursor for the preparation of **4** and **5**. In term of color change, compound **3** exhibited higher stability than **1** and **2** under ambient condition. A two-step reaction of **3** with excess 25% aqueous ammonium hydroxide and subsequently with concentrated hydrochloric acid gave cassiarin A hydrochloride **4a** in excellent yield (99%). The latter was further treated with 5% aqueous sodium carbonate solution to obtain compound **4** in quantitative yield (90%).

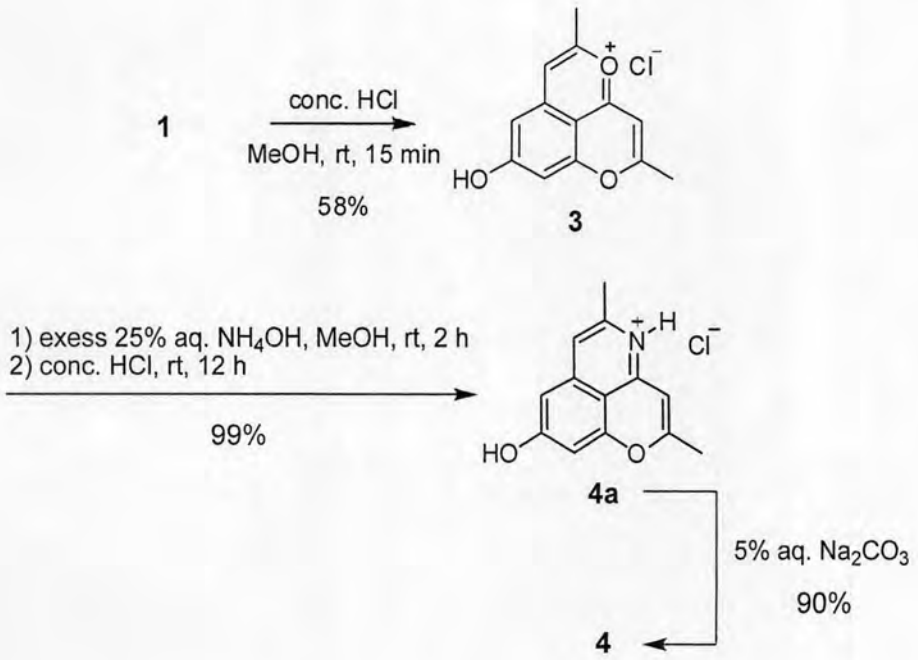

Scheme 4-10. Transformation of **1** into **4**.

It was proposed that recyclization of pyrylium ring of **3** was occurred via ring-opening and subsequent ring-closing mechanism [20] (Scheme 4-11). Firstly, the lone pair electron of ammonia attacks C-4 position of **3** to generate intermediate **A**. Then, the opening of dihydropyran ring in **A** leads to imine-enolate **B**, which exists in equilibrium with keto-enamine **C**. After that, the intramolecular recyclization of **C** is

performed by nucleophilic attack of amino group at carbonyl carbon to obtain intermediate **D**, which undergoes acid-catalyzed dehydration to give **4a**. Upon treatment of **4a** with Na_2CO_3, compound **4** was obtained.

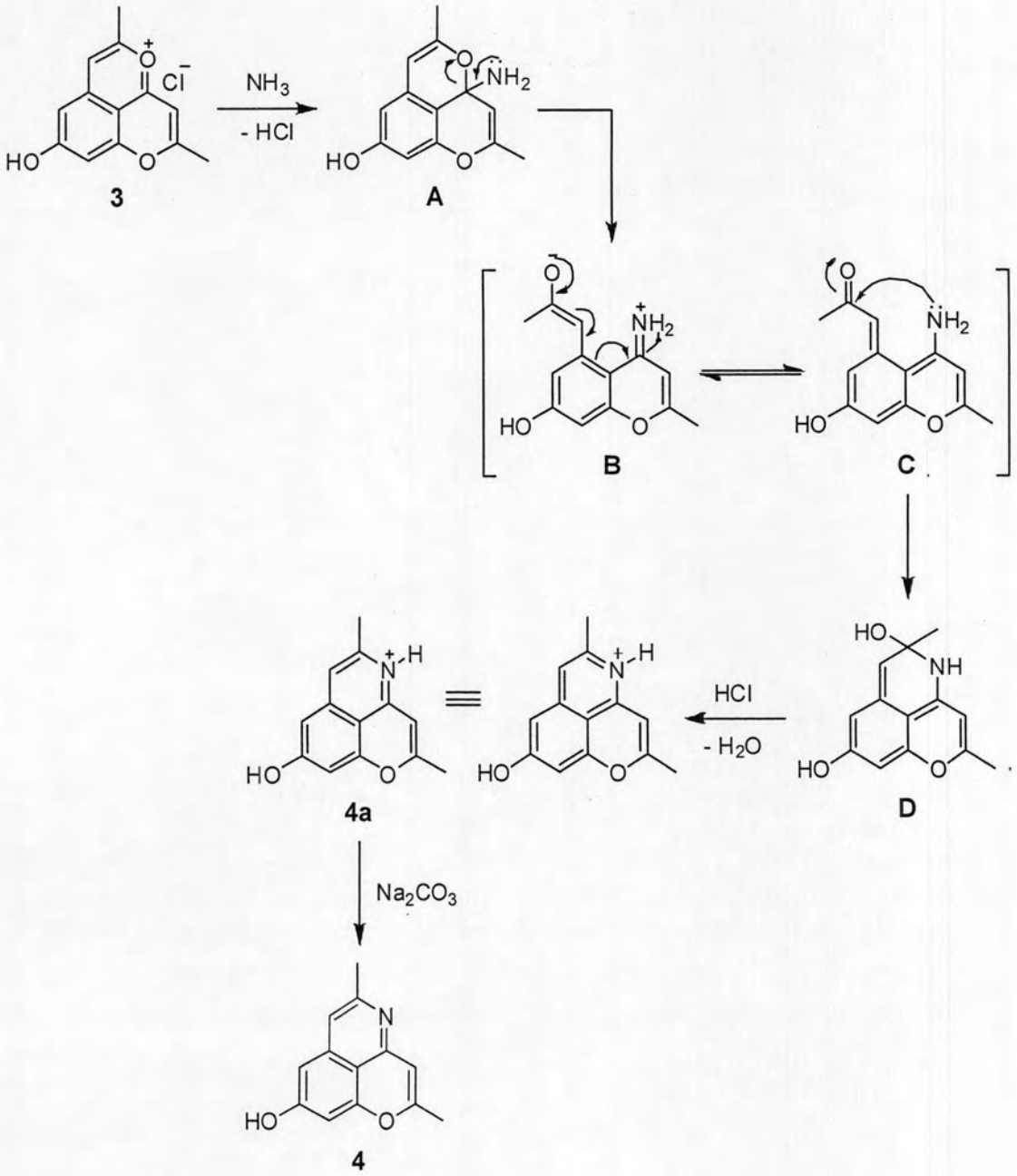

Scheme 4-11. A possible mechanism for synthesis of **4**.

The formation of synthetic **4** and **4a** was confirmed by ^{1}H- and ^{13}C-NMR spectroscopy and compared with the previously reported spectral data of natural **4** as shown in Table 4-1.

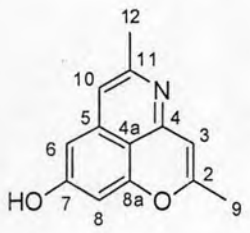

4

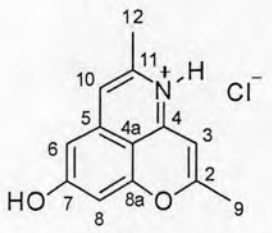

4a

Table 4-1. Chemical shift of ^{1}H- (δ_H, ppm) and ^{13}C-NMR (δ_C, ppm) data of **4** and **4a** compared with those of natural **4**.

Carbon No.	natural **4**[a]		**4a**[b]		synthetic **4**[c]	
	δ_H	δ_C	δ_H	δ_C	δ_H	δ_C
2		161.5		168.1		159.1
3	6.03 (s, 1H)	103.7	6.50 (s, 1H)	98.0	6.06 (s, 1H)	106.1
4		150.6		148.3		153.4
4a		111.5		109.4		111.7
5		138.8		138.1		138.4
6	6.46 (s, 1H)	102.9	6.85 (d, J = 1.6 Hz, 1H)	104.4	6.42 (s, 1H)	100.9
7		164.6		166.1		160.9
8	6.48 (s, 1H)	100.7	6.89 (d, J = 1.6 Hz, 1H)	101.1	6.45 (s, 1H)	99.1
8a		156.4		156.4		155.3
9	2.20 (s, 3H)	20.1	2.45 (s, 3H)	19.1	2.13 (s, 3H)	19.8
10	6.70 (s, 1H)	113.7	7.06 (s, 1H)	114.2	6.80 (s, 1H)	112.8
11		149.5		140.6		150.5
12	2.34 (s, 3H)	22.7	2.46 (s, 3H)	17.5	2.28 (s, 3H)	24.5

[a] obtained in $CDCl_3/CD_3OD$ (1:1) [12].

[b] obtained in CD_3OD.

[c] obtained in DMSO-d_6.

From Table 4-1, ^{1}H-NMR patterns of synthetic **4** and natural **4** are almost identical. Four singlet signals at δ_H 6.06 (1H), 6.42 (1H), 6.45 (1H) and 6.80 (1H) were assigned to the conjugated sp^2-methine protons (=CH−), while two singlet signals at δ_H 2.45 (3H) and 2.46 (3H) for methyl protons. ^{1}H-NMR signal of hydroxyl group (−OH) was not observed (Figure A-10). Compared to **4**, H-6 and H-7 of **4a** had shown two doublet signals at δ_H 6.89 (1H) and 6.85 (1H) with the same coupling constant (J = 1.6 Hz). This is attributed the present of meta-coupled phenolic protons, which was proved by HMBC correlation (Figure A-9). From the HMBC experiment, the proton H-6 (δ_H 6.89) and H-8 (δ_H 6.85) were correlated with δ_C 166.1 of C-7, whereas the proton H-3 (δ_H 6.50) and H-10 (δ_H 7.06) were correlated with δ_C 19.1 and 17.5 which were assigned to methyl carbons of C-9 and C-12, respectively. ^{13}C-NMR spectra of both synthetic **4a** (Figure A-7) and **4** (Figure A-11) contains 13 carbon signals due to seven quaternary sp^2 carbons, four sp^2 methine carbons and two methyl carbons, and consistent with those of natural **4**. Moreover, the formation of synthetic **4a** and **4** were further confirmed by the presence of strong molecular ion base peaks in HR-ESI-MS spectra at *m/z* 214.0882 ([M−Cl]$^+$ for **4a**, Figure B-1) and 214.0868 ([M+H]$^+$ for synthetic **4**, Figure B-2).

4.2 Synthesis of Cassiarin B (5)

In a similar manner to **4**, compound **5** was prepared from key precursor **3** via the formation of **5a** (Scheme 4-12). The use of *N*-methyl-4-aminobutyrate as an amine reagent to react with **3** afforded *N*-methoxy-4-oxobutyl cassiarin A chloride **5a** in 87% yield. The latter was further reacted with 5% aqueous sodium carbonate solution or triethylamine to give **5** in 60% yield.

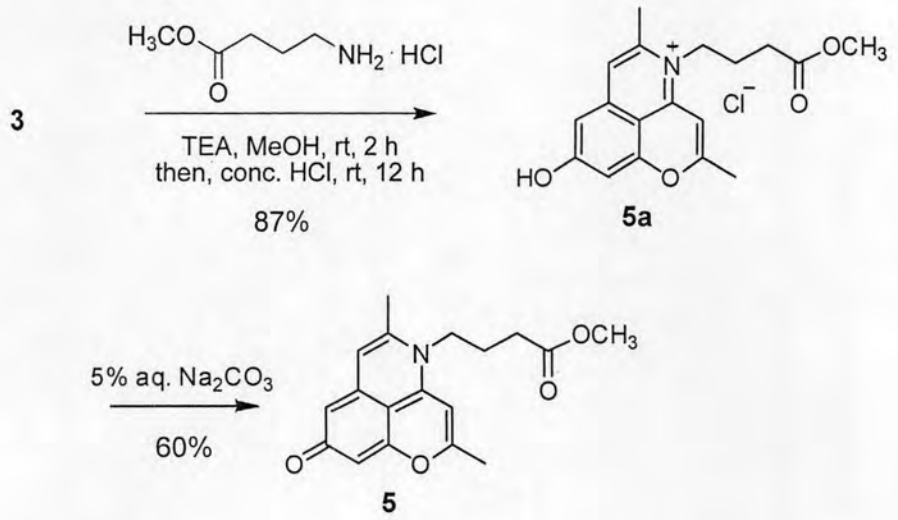

Scheme 4-12. Transformation of **3** into **5**

The correct structures of synthetic **5** and **5a** were verified by ^{1}H-NMR, ^{13}C-NMR, 2D-NMR (HSQC and HMBC) and MS experiments. Table 4-2 summarized the ^{1}H- and ^{13}C-NMR data of **5** and **5a** compared with natural **5**. In case of **5**, signals of three methylene proton groups were observed at δ_H 1.89−1.96 (m, 2H), 2.56 (t, J = 6.4 Hz, 2H) and 3.99 (t, J = 8.4 Hz, 2H). A singlet signal appeared at δ_H 3.71 (3H) indicating the present of methoxy proton group of ester. Four singlet signals at δ_H 6.22 (s, 1H), 6.35 (s, 1H), 6.59 (s, 1H) and 6.64 (s, 1H) were assigned to the conjugated sp^2 methine protons and two singlet signals at δ_H 2.37 (s, 3H) and 2.44 (s, 3H) for methyl protons (Figure A-16). For compound **5a**, ^{1}H-NMR spectrum was similar to that of **5** and ^{1}H-NMR signal of hydroxyl group was not observed (Figure A-12). The ^{13}C-NMR spectra of synthetic **5** and **5a** are similar and both revealed 18 carbon signals as expected.

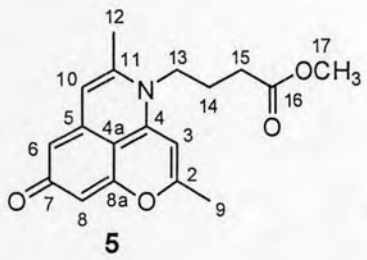

5

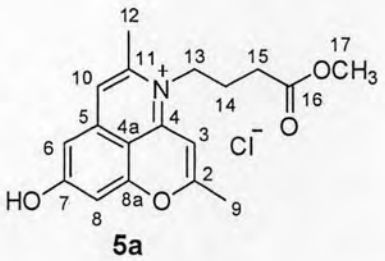

5a

Table 4-2. Chemical shift of ^{1}H- (δ_H, ppm) and ^{13}C-NMR (δ_C, ppm) data of **5** and **5a** compared with those of natural **5**

Carbon No.	natural **5**[a]		**5a**[b]		synthetic **5**[c]	
	δ_H	δ_C	δ_H	δ_C	δ_H	δ_C
2		168.0		169.1		166.0
3	6.74 (s, 1H)	97.3	6.54 (s, 1H)	97.1	6.59 (s, 1H)	95.7
4		148.6		148.7		146.8
4a		109.3		110.1		107.7
5		136.5		135.6		135.4
6	6.48 (s, 1H)	107.9	6.38 (d, J = 1.6 Hz, 1H)	103.8	6.22 (s, 1H)	106.9
7		174.6		163.5		177.7
8	6.60 (s, 1H)	105.1	6.48 (d, J = 2.0 Hz, 1H)	101.1	6.35 (s, 1H)	104.9
8a		156.7		155.0		155.8
9	2.43 (s, 3H)	21.0	2.28 (s, 3H)	20.1	2.37 (s, 3H)	19.3
10	6.78 (s, 1H)	117.1	6.76 (s, 1H)	116.7	6.64 (s, 1H)	115.1
11		141.4		142.6		140.1
12	2.50 (s, 3H)	20.2	2.36 (s, 3H)	19.2	2.44 (s, 3H)	18.6
13	4.10 (t, J = 8.5 Hz, 2H)	48.0	3.98 (t, J = 8.0 Hz, 2H)	47.7	3.99 (t, J = 8.4 Hz, 2H)	46.6
14	1.98 (m, 2H)	23.8	1.83–1.91 (m, 2H)	22.1	1.89–1.96 (m, 2H)	22.8
15	2.57 (t, J = 6.3 Hz, 2H)	30.3	2.47 (t, J = 6.6 Hz, 2H)	29.7	2.56 (t, J = 6.4 Hz, 2H)	29.1

Carbon No.	natural **5**[a]		**5a**[b]		synthetic **5**[c]	
	δ_H	δ_C	δ_H	δ_C	δ_H	δ_C
15	2.57 (t, J = 6.3 Hz, 2H)	30.3	2.47 (t, J = 6.6 Hz, 2H)	29.7	2.56 (t, J = 6.4 Hz, 2H)	29.1
16		174.4		175.4		173.5
17	3.72 (s, 3H)	52.3	3.55 (s, 3H)	52.2	3.71 (s, 3H)	50.9

[a] obtained in $CDCl_3/CD_3OD$ (1:1) [12].

[b] obtained in D_2O/DMSO-d_6 (9.5:0.5).

[c] obtained in CD_3OD.

The presence of conjugated carbonyl group in synthetic compound **5** was proved by HMBC correlation. From the HMBC data of compound **5a** (Figure A-12), the proton H-6 (δ_H 6.38) and H-8 (δ_H 6.48) were correlated with δ_C 163.5 of the phenolic carbon C-7. In case of **5**, proton H-6 (δ_H 6.22) and H-8 (δ_H 6.35) were correlated with the C-7 at δ_C 177.7, which was designated to the conjugated carbonyl carbon. Regards the formation mechanism of **5** from **5a**, it is likely that base firstly liberated hydroxyl proton of **5a** to generate phenolate ion **F** which subsequently underwent electron delocalization to form **5** (Scheme 4-13).

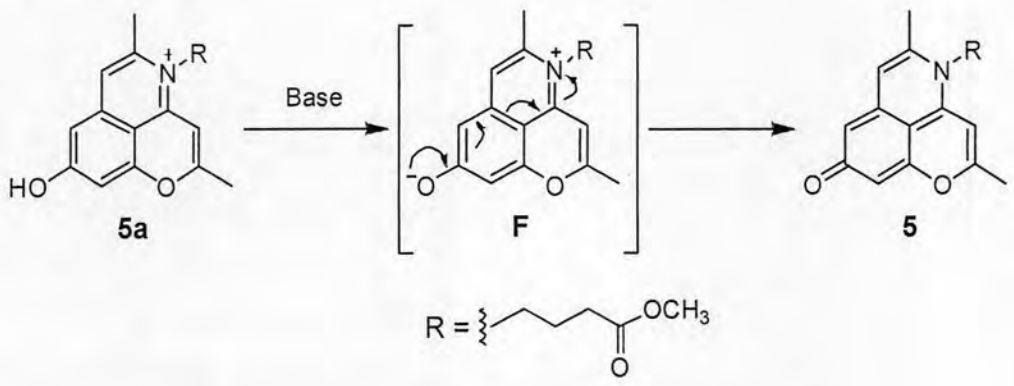

Scheme 4-13. Transformation mechanism from **5a** to **5.**

HR-ESI-MS spectra of **5** and **5a** exhibited strong molecular ion base peaks at *m/z* 314.1387 $[M+H]^+$ (Figure B-4) and 314.1382 $[M-Cl]^+$ (Figure B-3), respectively. In case of **5**, mass spectrum exhibited weak molecular ion peak at *m/z* 627.2751 $[2M-H]^+$.

A possible mechanistic pathway for **4** and **5** is proposed. Compound **4** and **5** could be derived from anhydrobarakol salt (**3**) or 5-acetonyl-7-hydroxy-2-methyl chromone (**27**), both of which were generate from barakol (**1**) and followed by cyclization of corresponding alkaloid chromone (Scheme 4-14).

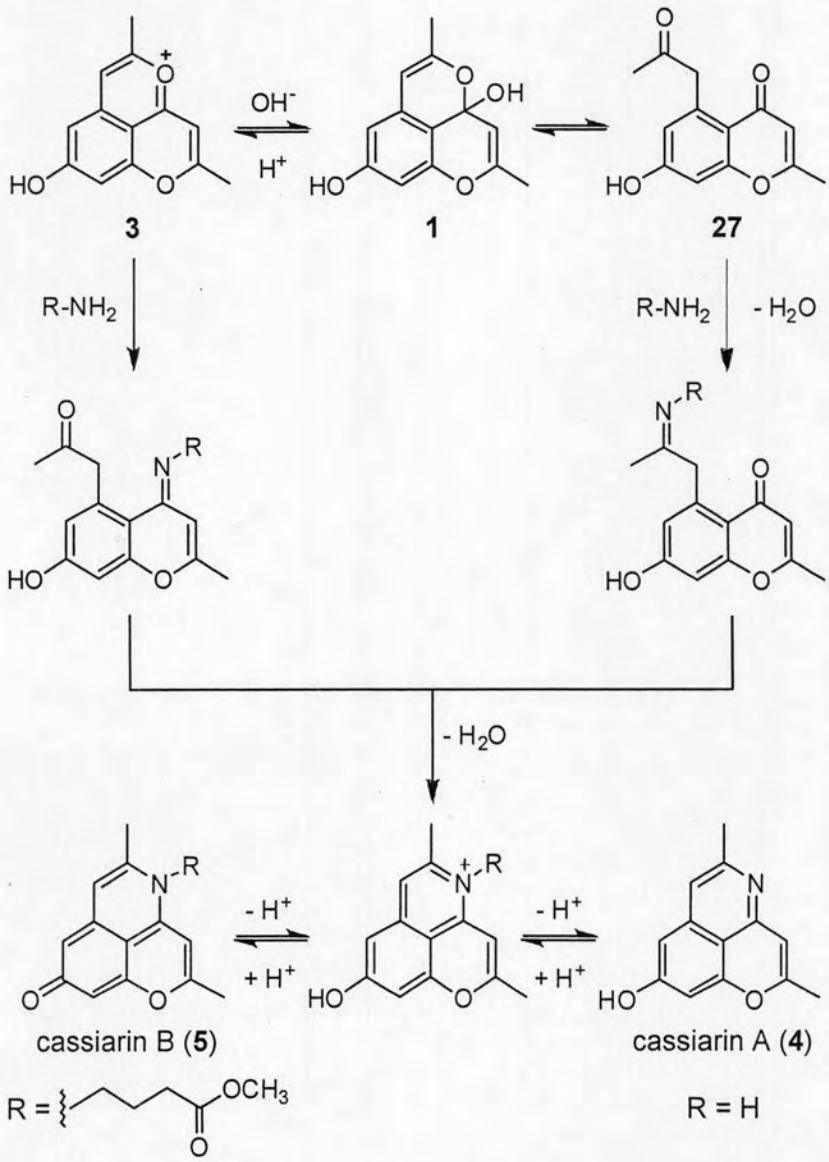

Scheme 4-14. A possible mechanistic pathway of **4** and **5**

4.3 Syntheses of *N*-Substituted Cassiarin Derivatives

The above-mentioned synthesis of **5a** from **3** proved itself as a key route for the synthesis of new cassiarin derivatives bearing a different *N*-substituent. In this part, the preparation of derivatives containing straight-chain alkyl (i.e. *n*-butyl), bulky alkyl (i.e. cyclohexyl), phenyl or benzyl group is demonstrated.

Firstly, compound **3** was reacted with an appropriate amine to give the corresponding *N*-substituted cassiarins **28a–31a** in 76 89% yield (Table 4-3). The lower yield of compound **30a** compared to that of other derivatives is attributed to reduced basicity and nucleophilicity of aniline (entry 5, Table 4-3) [17]. Subsequently, treatment of compound **28a–31a** with triethylamine in aqueous solution leaded to transformation to their neutral forms **28b–31b** in good yield (65 87%) without chromatographic purification.

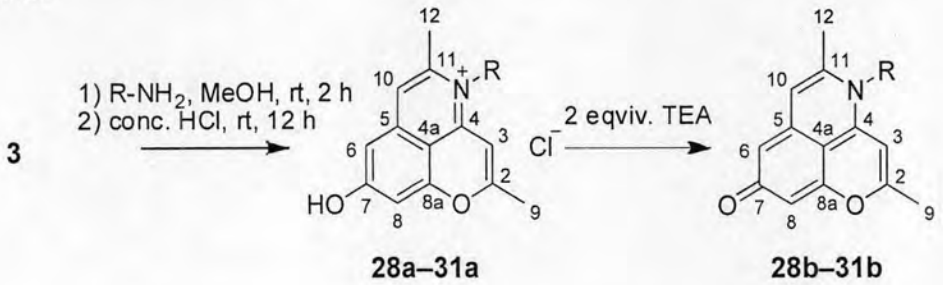

Table 4-3. Syntheses of *N*-substituted cassiarin derivatives.

Entry	R	Compound	yield (%)
1	*n*-Butyl	**28a**	88
2	*n*-Butyl	**28b**	67
3	Cyclohexyl	**29a**	87
4	Cyclohexyl	**29b**	67
5	Phenyl	**30a**	76
6	Phenyl	**30b**	65
7	Benzyl	**31a**	89
8	Benzyl	**31b**	87

The formation of all cassiarin derivatives were confirmed by ^{1}H-NMR, ^{13}C-NMR, HSQC, HMBC and MS techniques. Structural elucidation of each compounds are described below.

Compound **28a** and **28b**: ^{1}H-NMR spectra (Figure A-20 for **28a** and Figure A-36 for **28b**) showed a triplet signal of methylene proton adjacent to the nitrogen atom at δ_H 4.20 (J = 8.0 Hz) and 3.96 (J = 8.0 Hz), respectively. Multiplet signals of two residual methylene proton groups were appeared at δ_H 1.44−1.53, 1.67−1.75 for **28a** and 1.43−1.53, 1.61−1.68 for **28b**. Then, the terminal methyl proton group was shown the triplet signal at δ_H 0.98 (J = 8.0 Hz) for **28a** and 1.02 (J = 4.0 Hz) for **28b**. Compared to **28b**, the alkyl protons of **28a** gave more downfielded signals due to inductive effect. This is affected from the positive charge of nitrogen atom in **28a**. ^{13}C-NMR spectra of **28a** (Figure A-21) and **28b** (Figure A-37) revealed 17 carbon signals, and a signal of hydroxylic carbon on phenol ring of **28a** was shown at δ_C 165.4, while that of a conjugated carbonyl carbon of **28b** appeared at δ_C 177.7, which were proved by HSQC and HMBC correlation (Figure A-22 and A-23 for **28a**, and Figure A-38 and A-39 for **28b**, respectively). A molecular ion base peak in HR-ESI-MS spectra was observed at *m/z* 270.1531 $[M-Cl]^+$ for **28a** (Figure B-5) and 270.1538 $[M+H]^+$ for **28b** (Figure B-9). In case of **28b**, mass spectrum exhibited a weak fragment peak at *m/z* 214.0919, which was consistent with the loss of a *n*-butyl group.

Compound **29a** and **29b**: their ^{1}H-NMR spectra (Figure A-24 for **29a** and Figure A-40 for **29b**) showed multiplet signals in range of δ_H 1.21 to 2.41 (10H), which were assigned to methylene protons of cyclohexyl ring. A signal of sp^3-methine proton was indicated at δ_H 4.61 for **29a** and 4.36 for **29b**. Similarly, to the above-mentional data, deshielding effect was observed in **29b** due to the inductive ammonium group. ^{13}C-NMR spectra of **29a** (Figure A-25) and **29b** (Figure A-41) revealed 19 carbon signals. From HSQC and HMBC correlations (Figure A-26 and A-27 for **29a**, and Figure A-42 and A-43 for **29b**, respectively), a signal of hydroxylic carbon on phenol ring of **29a** was observed at δ_C 165.9 and that of a conjugated carbonyl carbon of **29b** was appeared at δ_C 178.4. These compounds showed a molecular ion base in the HR-ESI-MS peak at *m/z*

296.1674 $[M-Cl]^+$ for **29a** (Figure B-6) and 296.1676 $[M+H]^+$ for **29b** (Figure B-9). Mass spectra of both **29a** and **29b** exhibited a fragment peak at *m/z* 214.0913 and 214.0912, respectively, which were consistent with the loss of cyclohexyl group. In case of **29b**, mass spectrum also exhibited a weak molecular ion peak at *m/z* 591.3263 $[2M-H]^+$.

Compound **30a** and **30b**: their ^{1}H-NMR spectra (Figure A-28 for **30a** and Figure A-44 for **30b**) showed multiplet signal assigned to a phenyl ring in the rage of δ_H 7.45 to 7.77 (5H). H-3 signal of **30a** appeared at more downfielded region than **30b**, which indicates that the phenyl ring of **30a** is affected by the anisotropic effect to H-3. ^{13}C-NMR spectra (Figure A-29 for **30a** and Figure A-45 for **30b**) revealed 19 carbon signals. A signal of hydroxylic carbon on phenol ring of **30a** was observed at δ_C 166.3 and that of a conjugated carbonyl carbon of **30b** was observed at δ_C 178.4, which were proved by HSQC and HMBC correlation (Figure A-30 and A-31 for **30a**, and Figure A-46 and A-47 for **30b**, respectively). These compounds showed a molecular ion base in the HR-ESI-MS peak at *m/z* 290.1110 $[M-Cl]^+$ for **30a** (Figure B-7) and 290.1137 $[M+H]^+$ for **30b** (Figure B-11).

Compound **31a** and **31b**: ^{1}H-NMR spectrum of **31a** (Figure A-32) showed multiplet proton signal in the rage of δ_H 7.35 to 7.43 (3H) and doublet signals at δ_H 7.15 (J = 7.2 Hz, 2H), which were assigned to the phenyl protons. Singlet signal at δ_H 5.64 (2H) was indicated to the methylene proton in benzyl side chain on nitrogen atom. Similarly, ^{1}H-NMR spectrum of **31b** (Figure A-48) appeared multiplet signal in the rage of δ_H 7.30 to 7.40 (3H) and a doublet signal at δ_H 7.10 (J = 7.6 Hz, 2H) for phenyl protons. A singlet proton at δ_H 5.38 (2H) was assigned to the methylene protons of benzyl group. For ^{13}C-NMR, HSQC and HMBC data, each ^{13}C-NMR spectrum (Figure A-33 for **31a** and Figure A-49 for **31b**) revealed 19 carbon signals. A signal of hydroxylic carbon on phenol ring of **31a** was observed at δ_C 166.0 and that of a conjugated carbonyl carbon of **31b** was observed at δ_C 178.3, which were proved by HSQC and HMBC correlation (Figure A-34 and A-35 for **31a**, and Figure A-50 and A-51 for **31b**, respectively). These compounds showed a molecular ion base in the HR-ESI-

MS peak at *m/z* 304.1365 $[M-Cl]^+$ for **31a** (Figure B-8) and 304.1365 $[M+H]^+$ for **30b** (Figure B-12). Mass spectra of both **31a** and **31b** exhibited a fragment peak at *m/z* 213.0869 and 213.0869, respectively, which was consistent with the loss of benzyl group. In case of **31b**, mass spectrum exhibited a weak molecular ion peak at *m/z* 607.2601 $[2M-H]^+$.

4.4 Biological Activities

4.4.1 Antiplasmodial Activity

Antiplasmodial activity of all synthetic compounds was evaluated against a *Plasmodium falciparum* (K1, multi drug resistant strain). All synthetic cassiarin derivatives **5a**, **28a–31a** and **28b–31b** were inactive (%inhibition < 50%). These results suggest that side chain, which had bulky and/or hydrophobic substituents on nitrogen atom affect to the structural activity relationship (SAR) by reduced an activity. In case of analog **5a** compared with natural **5**, antiplasmodial activity may be decreased by induced inductive property of core structure.

4.4.2 Cytotoxic Activity

The *in vitro* cytotoxic activity of all synthetic cassiarin derivatives against 6 cell lines, including SW620 (colon), BT474 (breast), KATO-III (gastric), Hep-G2 (hapatoma), Chago (lung) and CH-Liver (liver) cancer, which were determined in percentage of survival (PS) was reported in Table 4-4. The results from Table 4-4 showed that all synthetic cassiarin derivatives **4**, **4a**, **5**, **5a**, **28a–31a** and **28b–31b** were inactive (PS > 50%).

Table 4-4. Cytotoxic activity against cell line of all synthetic cassiarin derivatives

entry	compound	Percentage of Survival (PS, %)[a]					
		SW620 (colon)	BT474 (breast)	KATO-III (gastric)	Hep-G2 (hepatoma)	Chago (lung)	CH-Liver (liver)
1	**4**	79	100	72	84	101	96
2	**5**	100	94	92	103	103	92
3	**4a**	86	102	106	120	101	90
4	**5a**	98	94	73	82	102	92
5	**28a**	97	97	80	85	103	91
6	**29a**	90	104	71	83	104	81
7	**30a**	93	81	99	111	103	80
8	**31a**	97	95	76	89	102	88
9	**28b**	100	106	103	104	105	106
10	**29b**	98	97	136	152	104	100
11	**30b**	99	103	137	150	104	111
12	**31b**	96	90	138	134	104	90

[a] average value